

Blast-Induced Failure of Steel Base Plate-Column Connections

Ahmed M. Abd-El-Latif^{1*}, Kareem Mohamed Salaheldin²

¹ Teaching assistant, Civil Engineering Department, Giza Engineering Institute, Giza, Egypt. E-mail: Ahmed.Abdlatif@gei.edu.eg, ORCID: <https://orcid.org/0009-0005-3953-4581>

² Lecturer, Civil Engineering Department, Giza High Institute of Engineering and Technology, Giza, Egypt. E-mail: salaheldin.k.m@gmail.com, ORCID: <https://orcid.org/0009-0001-7842-4829>
icets25@gei.edu.eg

Corresponding author: Ahmed M. Abd-El-Latif (Ahmed.Abdlatif@gei.edu.eg).

Received 09-09-2024

Revised 10-10-2024

Accepted: 1-11-2024

Published: July-2025

Copyright © 2021 by author(s) and
Journal Of Engineering Advances And Technology
For Sustainable Applications
This work is licensed under the Creative
Commons Attribution International
License (CC BY 4.0).

<http://creativecommons.org/licenses/by/4.0/>



Open Access

Print ISSN: 3062-5629
Online ISSN: 3062-5637

Abstract- Base plate-column connections BPCC are critical structural elements that transfer loads between various structural components. Their performance under extreme loading conditions, such as blast, is paramount for ensuring structural integrity. This study utilizes finite element analysis (FEA) to numerically examine the dynamic response of steel-to-concrete bolted connections SCBC and steel-to-steel welded connections SSWC subjected to blast loads of varying intensities.

A comprehensive three-dimensional finite element model was developed using the Coupled Eulerian-Lagrangian (CEL) method within the ABAQUS/CAE software. Realistic material properties were assigned to the steel, concrete, and TNT explosive components to accurately simulate the structural response. The model was subjected to blast loads generated by TNT charges of 200 kg and 500 kg, positioned at a standoff distance of 2.0 meters.

The numerical simulations yielded valuable insights into the deformation patterns, stress distributions, and failure modes of the connections under blast loading. The results demonstrated that the connection's response was significantly influenced by the magnitude of the blast load and the connection's rigidity. This research contributes to a deeper understanding of the blast resistance of steel-to-steel welded connection and steel-to-concrete bolted connections. The findings can be leveraged to inform design guidelines and mitigation strategies for structural systems exposed to blast threats.

Keywords- Coupled Eulerian-Lagrangian, blast loading, Connections.

1. INTRODUCTION

Steel structures rely heavily on connections to ensure their structural integrity and functional performance. Historically, a variety of connection types, including bolted, riveted, welded, and hybrid solutions, have been implemented. However, welded and bolted connections have dominated the field since the 1930s [1]. The continual drive for improved structural performance and economic efficiency has spurred the development of innovative connection technologies. Steel structures offer distinct advantages, such as ease of construction and deconstruction, often attributed to the modular nature of their components. This modularity enables efficient assembly and disassembly, facilitating potential reuse and recycling of materials. As structural members are interconnected, they are subjected to a range of forces, encompassing axial, bending, and shear loads. [1]

Base plate-column connections (BPCCs), a prevalent connection type in steel construction, typically involve a plate

welded to the base of the steel column member and anchored into a concrete foundation utilizing bolts. These connections are primarily designed to transfer superstructure loads, including axial forces, shear forces, and bending moments, to the foundation. As the final link in the load transfer path between the superstructure and the foundation, BPCCs play a critical role in ensuring the overall structural integrity. The design of the column base, composed of various elements, must adhere to the strength and stiffness requirements outlined in relevant design codes. In recent years, numerous experimental and numerical investigations have been conducted to gain a broader perspective of the structural behavior of these connections [4].

Column base plate-column connections (BPCCs) comprise several components, including the steel column, base plate, anchor rods, and pedestal concrete column [5], each of which influences the connection's competence to resist superstructure stresses. Figure (1) shows the main components of the column base plate-column connections (BPCCs). Figure 1 illustrates the primary strands of Base plate-column connections

(BPCCs).

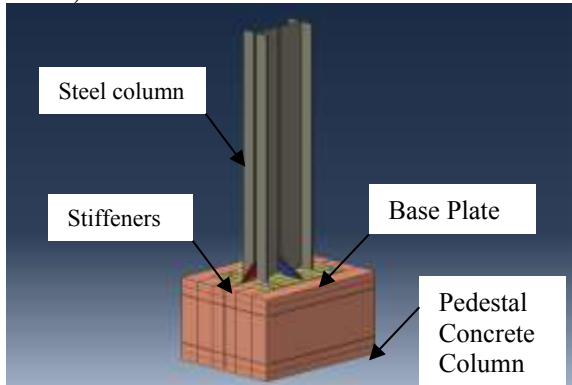


Figure (1): Base plate-column connection

Column Base Plate-Column Connections have been the subject of numerous experimental and numerical investigations to identify the primary failure modes base on different static loading scenarios, including anchor rod Rupture, base plate Misshapen, and concrete foundation crushing [6].

Additionally, while numerous studies have investigated Base Plate-Column Connections (BPCCs) under static loading conditions, exploring their structural behavior under dynamic loads, particularly implosive loads, remains relatively unexplored.

Recent decades have witnessed an upsurge in scholarly participation in the structural behavior under blast loading conditions, mostly driven motivated by the escalating incidence of terrorist attacks worldwide. The catastrophic failures observed in structures like the World Trade Center (1993) and the Murrah Federal Building (1995) underscored the devastating implications of inadequate blast resistance, with structural collapse often surpassing the immediate blast effects in terminology of casualties and injuries [7]. Traditional building designs, frequently centered around moment-resisting frames, are ill-equipped to withstand the sudden, intense forces generated by explosions. These loads, orders of magnitude greater than service loads and delivered within milliseconds, can induce catastrophic international failures. For instance, a fairly small 4530 gm TNT charge detonated at a distance of 15240 mm can create peak pressures of approximately 0.1724 Bar over an exceptionally short duration [8].

Effective analysis and formulation of blast-resistant buildings necessitate a thorough understanding of blast phenomena, structural dynamics, and performance requirements. However, the intrinsic unpredictability of threats precludes the formulation of completely invulnerable structures. Consequently, a crucial of blast-resistant architecture involves establishing acceptable proportions of structural damage based on predefined safety goals [9].

This research endeavors to elucidate the intricate structural behavior of Base Plate-Column Connections (BPCCs) when subjected to implosive loading scenarios. The investigation will leverage the power of Coupled Eulerian-Lagrangian (CEL) computational techniques to simulate the dynamic response of these critical connections. A primary focus will be on discerning the profound influence exerted by the stiffness characteristics of both the steel-to-steel interface within the BPCC itself and the steel-to-concrete interface where anchor rods embed into the surrounding concrete. This multifaceted approach will provide valuable insights into the connection's capacity to withstand implosive loads, contributing to a deeper understanding of the factors that govern its dynamic behavior and ultimately enhancing the resilience of structures under such extreme loading conditions.

II. NUMERICAL VERIFICATION

To perform finite element analysis, Complete Abaqus Environment was employed. The Coupled Eulerian-Lagrangian (CEL) technique was employed, modeling the steel components using Lagrangian elements and the explosive material (TNT) and surrounding air using Eulerian elements. The model was developed based on the work of Abdellatif et al. 2024 [10], and the results were validated against their findings to ensure accuracy as illustrated in figures 2 and 3.

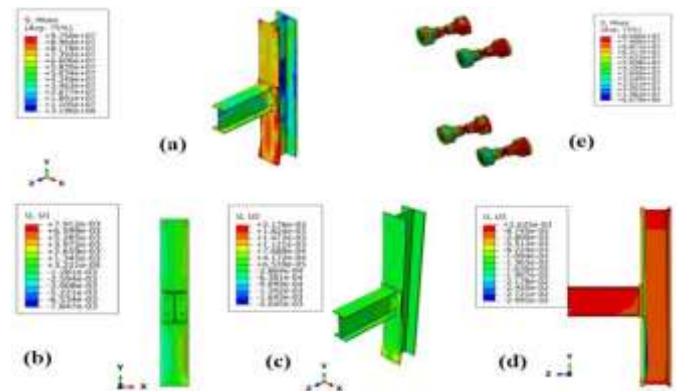


Figure (2): Stress and Deformation Contours for 10 kg TNT at 2.5 m Standoff (after Abdellatif et al. 2024 [7])

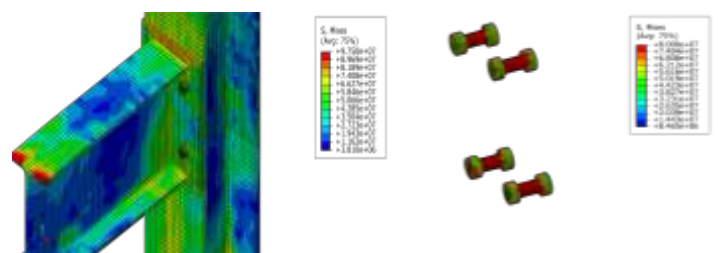


Figure (3): Calibration of Stress and Deformation Contours for 10 kg TNT at 2.5 m Standoff (after Abdellatif et al. 2024 [7])

10 kg TNT at 2.5 m Standoff

Coupled Eulerian-Lagrangian (CEL) approach effectively captures the interaction between the different model materials, particularly in large deformation scenarios, and accounts for blast waves reflections, enhancing simulation realism. The Column Base Plate-Column Connections (BPCCs) were subjected to blast waves generated by 200 kg, and 500 kg TNT charges at a standoff distance of 2.0 m.

III. MODEL GEOMETRIC CHARACTERISTICS

The Plate-Column connection (BPCCs) comprised an IPE 300 beam-column of 3000 mm length welded to a 20 mm thick steel plate. In certain models, stiffeners measuring 200 mm x 80 mm x 20 mm were incorporated to enhance the connection rigidity between the steel column and plate. High-strength steel bolts of 20 mm diameter were employed to anchor the steel plate to a concrete pedestal column measuring 700 mm x 550 mm x 1000 mm. The parametric study focused on the influence of stiffener presence and bolt quantity and the quantity of the TNT on the connection's behavior. as illustrated in figure 4.

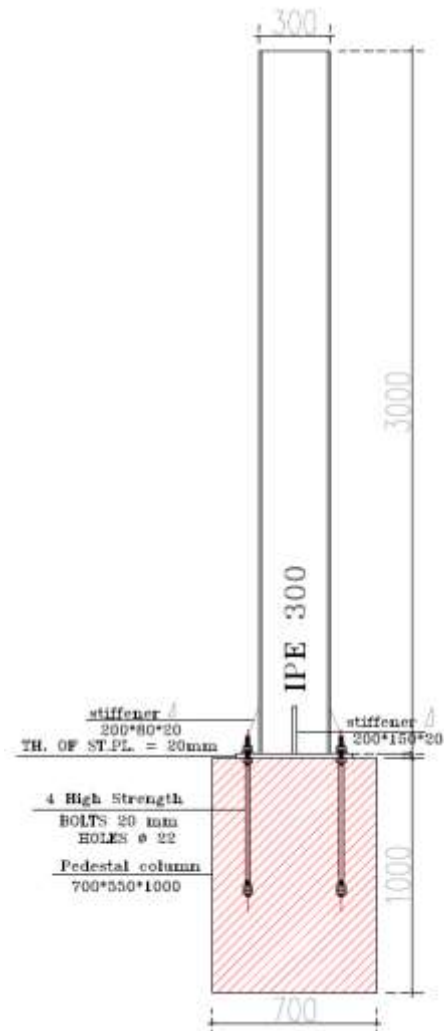


Figure (4): Base plate-column connection geometry

IV. CONSTITUTIVE MATERIAL MODELS

The concrete behavior was simulated using the Concrete Damaged Plasticity (CDP) model implemented in Abaqus. The model's material properties were calibrated to represent 25000 KPa compressive strength concrete [8]. The stress-strain relationship for the CDP model is given by:

$$\sigma_t = (1 - dt) E_0 (\epsilon_t - \tilde{\epsilon}_t^{pl}) \quad (1)$$

$$\sigma_c = (1 - dc) E_0 (\epsilon_c - \tilde{\epsilon}_c^{pl}) \quad (2)$$

Where: σ_c and σ_t are the compressive and tensile concrete stresses; dc and dt are the compressive and tensile damage factor; ϵ_c and ϵ_t are the concrete compressive and tensile strains; E_0 is the initial modulus of elastic of concrete.

The stress-strain behavior of the reinforcement steel within the concrete pedestal column and steel column was defined using the Johnson-Cook (JC) plasticity model for 520 MPa ultimate strength steel, as described in reference [11]. Grade 8.8 bolts, with yield and ultimate stresses of 834 MPa and 951 MPa,

respectively, were employed in the model.

V. MODEL MESH CHARACTERISTICS

Numerical simulations were performed on the reference BPCC models using the standard solver in “Abaqus Environment software”. A mesh sensitivity analysis was conducted to determine the optimal element size. A mesh size of 20 mm was adopted for the steel column, stiffeners, and steel plate, ensuring accurate representation of the interaction between these components. The reinforcement bars, stirrups and steel bolts were discretized with mesh sizes of 40 mm, 20 mm, and 10 mm, respectively. The reinforcement was embedded within the concrete column to simulate the bond between the two materials. The analysis calculated stresses and displacements in all directions. Figures 5a, and 5b demonstrate the mesh shape implied in the models.

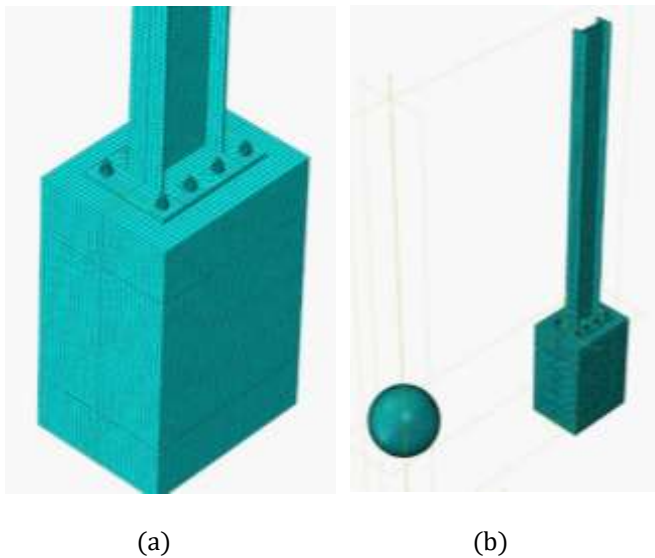


Figure (5): Finite Element Mesh of the Column Base Plate-Column Connection

VI. FINITE ELEMENT SIMULATION RESULTS

Six models were developed to investigate the impact of stiffener presence, bolt quantity, and TNT charge mass on the connection's behavior. Table 1 provides a detailed description of the parameters considered in each model.

Table (1): Models Characteristics

Model	TNT Charge	No. of bolts	Stiffeners
A	200 Kg	4	N.A
B	200 Kg	8	N.A
C	200 Kg	4	4
D	500 Kg	4	N.A
E	500 Kg	8	N.A
F	500 Kg	4	4

Figures 6-11 illustrate the typical time-history of deformation resulting from blast loading.

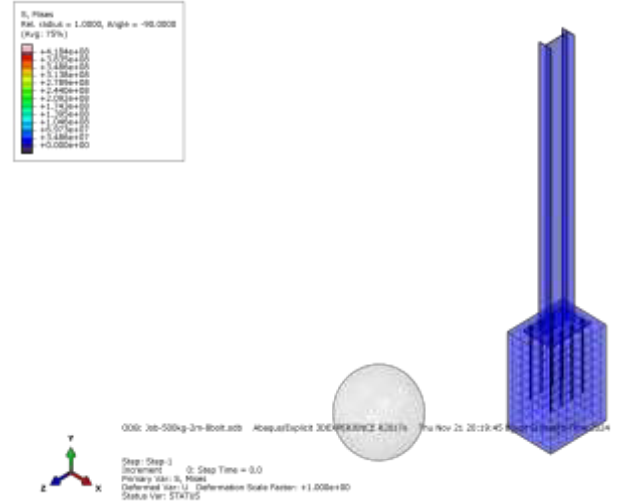


Figure (6): The Plate-Column connection (BPCCs) at step time 0.00 second

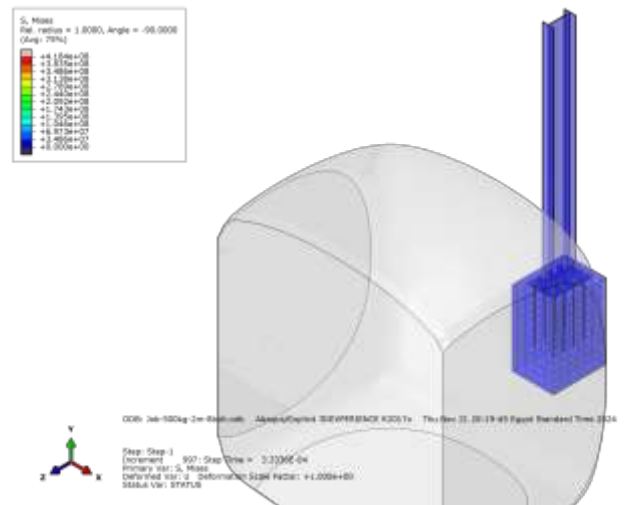


Figure (7): The Plate-Column connection (BPCCs) at step time 0.000333 second

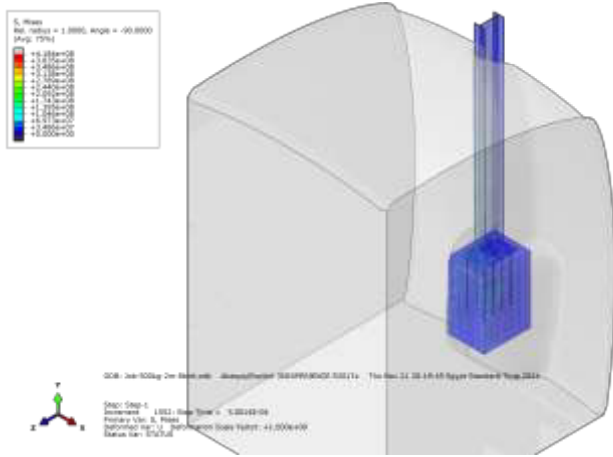


Figure (8): The Plate-Column connection (BPCCs) at step time 0.0005 second

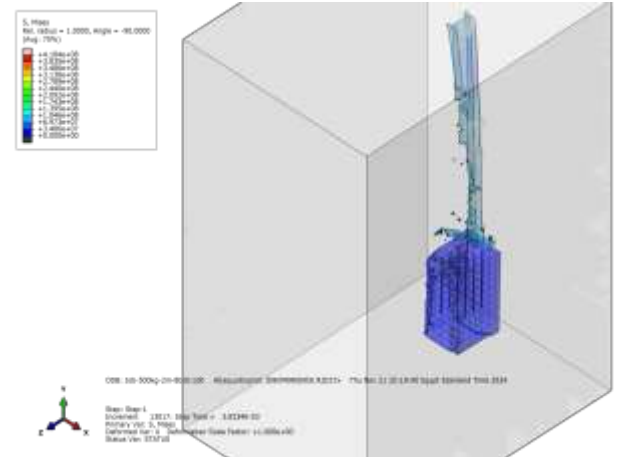


Figure (11): The Plate-Column connection (BPCCs) at step time 0.003833 second

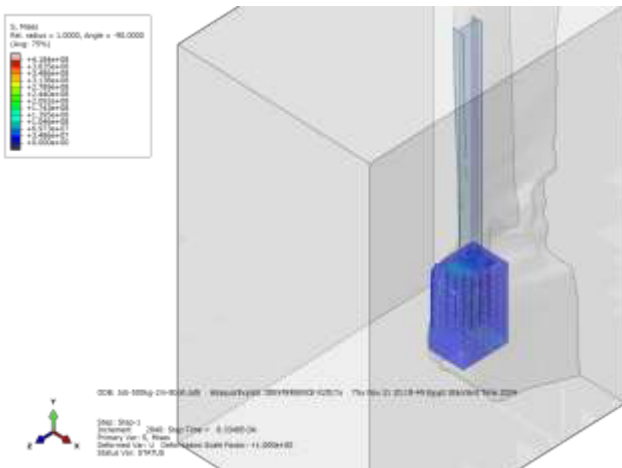


Figure (9): The Plate-Column connection (BPCCs) at step time 0.0008333 second

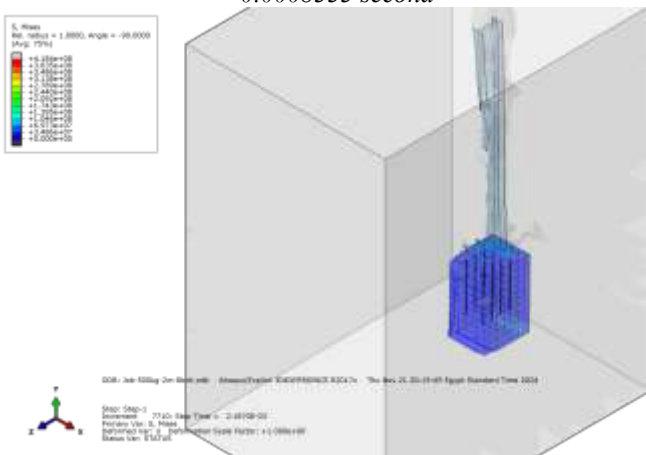
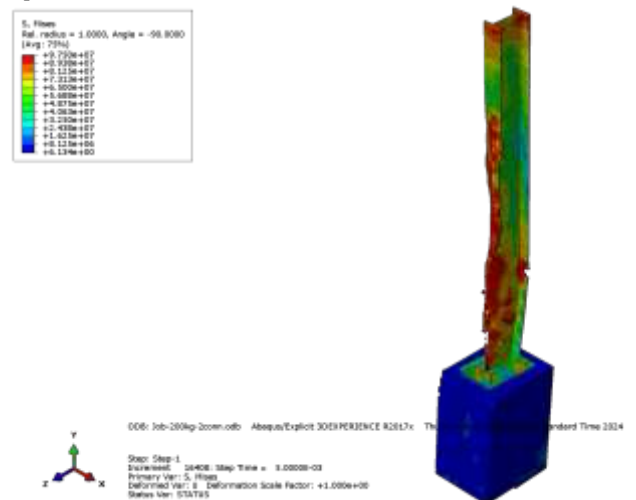


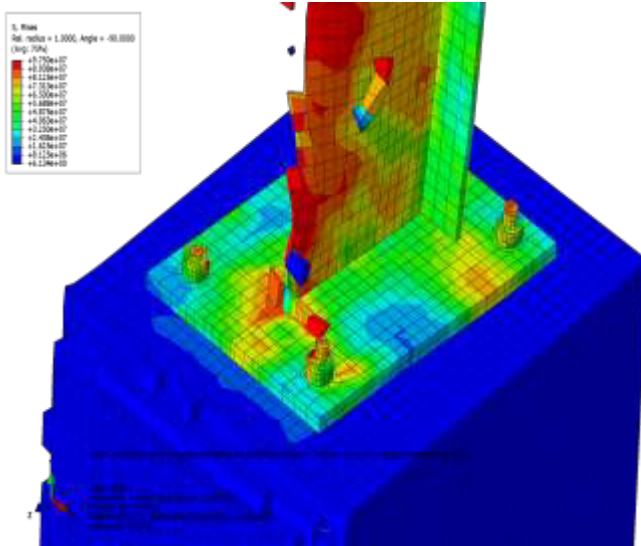
Figure (10): The Plate-Column connection (BPCCs) at step time 0.002167 second

Model (A):

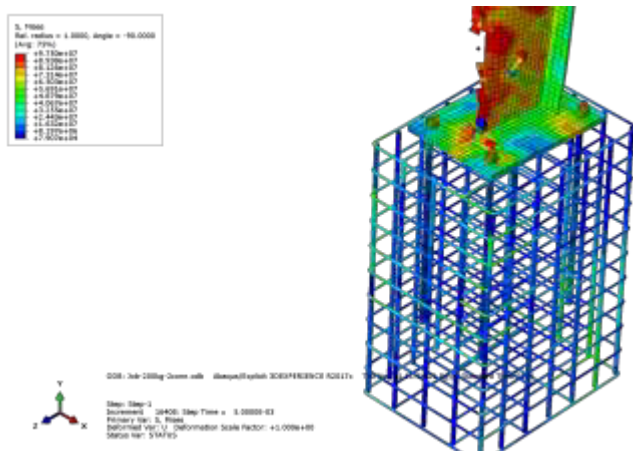
The BPCC was subjected to a blast wave generated by a 200 kg TNT charge at a standoff distance of 2 m. The blast loading resulted in moderate damage to the connection, without causing any significant deformation to the base plate or the pedestal column. However, the first two bolts facing the blast wave were damaged. Figures 11, 12, 13, and 14 illustrate the generated stresses of the connection from different perspectives.



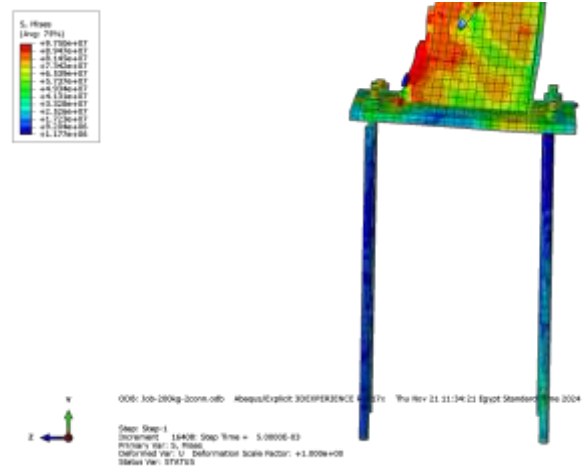
Figures (11): Global stress contour plot for the BPCC Subjected to blast loading for model (A)



Figures (12): Stress contour plot focusing on the BPCC connection for model (A)



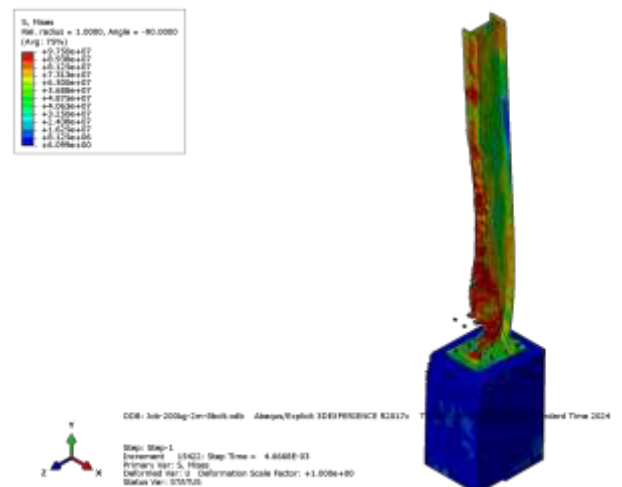
Figures (13): Stress contour plot for the BPCC connection and reinforcement within the concrete for model (A)



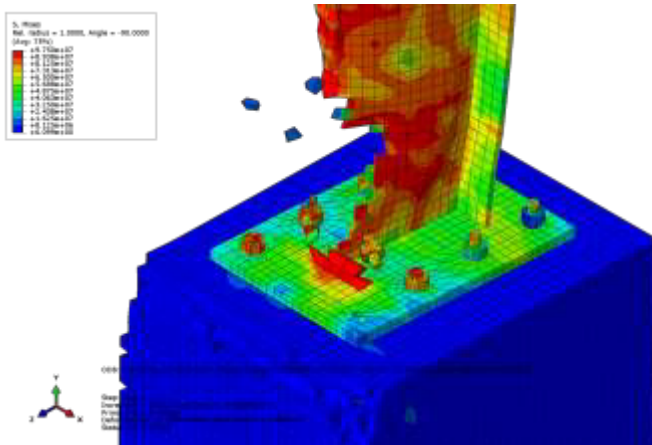
Figures (14): Stress contour plot focusing on the anchor bolts for model (A)

Model (B):

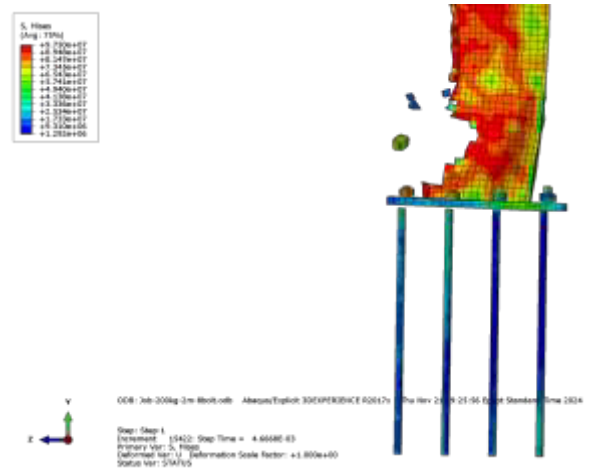
The BPCC was subjected to a blast wave generated by a 200 kg TNT charge at a standoff distance of 2 m. This model was similar to Model A, except for the increased number of bolts from 4 to 8. The blast loading resulted in moderate damage to the connection, with a slightly less deformation observed in the base plate and the rear bolts compared to Model A. However, the bolts facing the blast wave were still damaged. Some cracks were noticed in the pedestal concrete column. Figures 15, 16, 17, and 18 illustrate the stress distribution within the connection from different perspectives.



Figures (15): Global stress contour plot for the BPCC Subjected to blast loading for model (B)



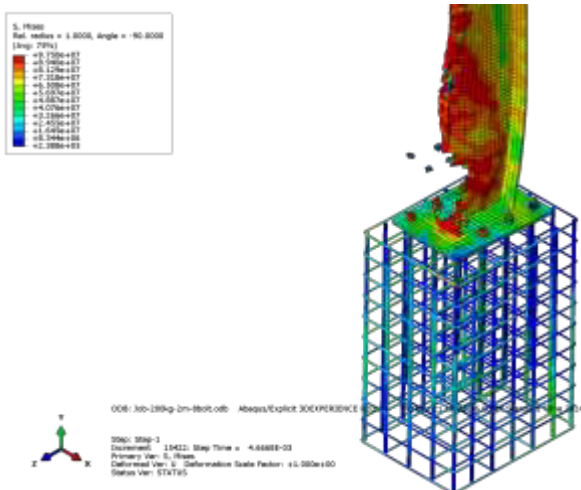
Figures (16): Stress Contour Plot focusing on the BPCC connection for model (B)



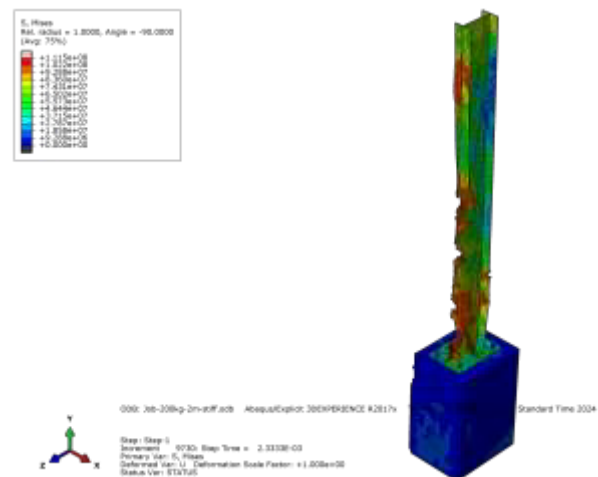
Figures (18): Stress contour plot focusing on the anchor bolts for model (B)

Model (C):

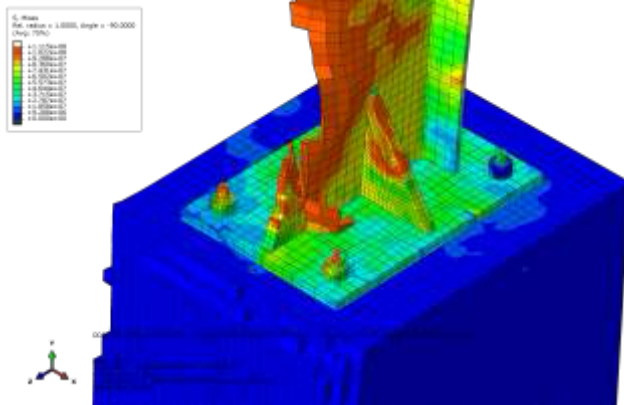
The BPCC was subjected to a blast wave generated by a 200 kg TNT charge at a standoff distance of 2 m. This model was similar to Model A, with the addition of stiffeners. The stiffeners induced a redistribution of stresses on the base plate as shown in figures 20, and 22, resulting in a significant reduction in deformation of the front bolts. But still Some cracks were noticed in the pedestal concrete column. Figures 19, 20, 21, and 22 illustrate the stress distribution within the connection from different perspectives.



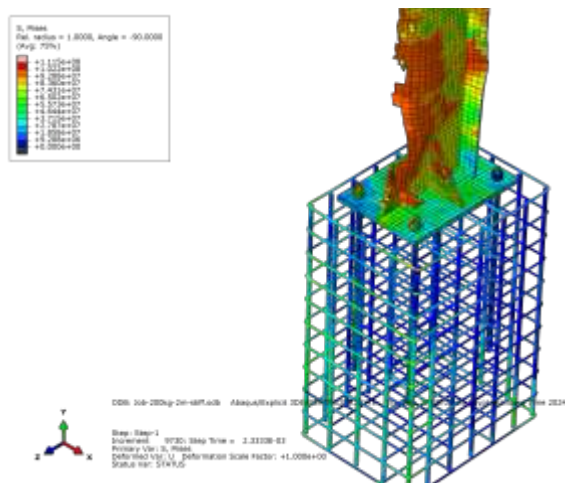
Figures (17): Stress contour plot for the BPCC connection and reinforcement within the concrete for model (B)



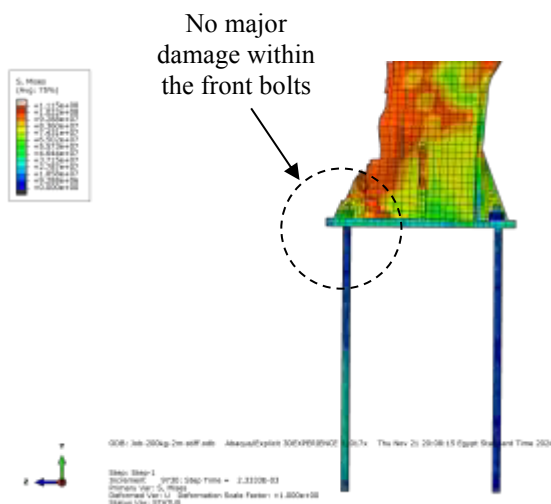
Figures (19): Global stress contour plot for the BPCC Subjected to blast loading for model (C)



Figures (20): Stress contour plot focusing on the BPCC connection for model (C)



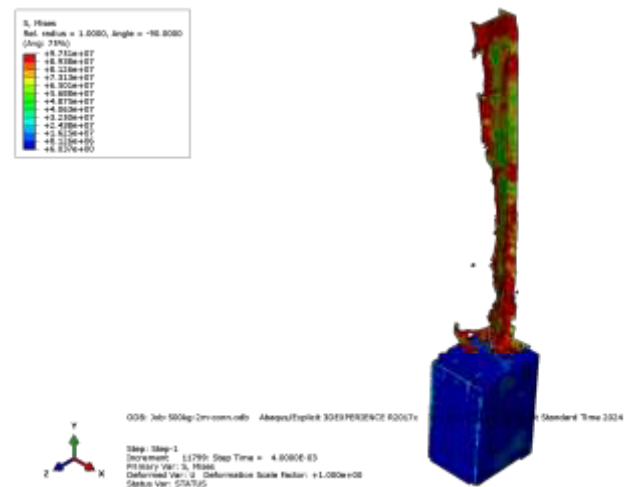
Figures (21): Stress contour plot for the BPCC connection and reinforcement within the concrete for model (C)



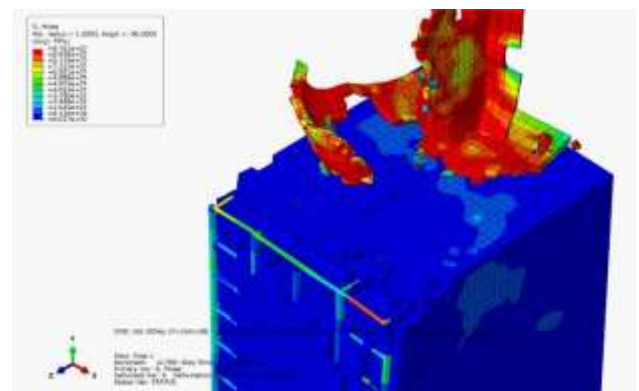
Figures (22): Stress contour plot focusing on the anchor bolts for model (C)

Model (D):

The BPCC was subjected to a blast wave generated by a 500 kg TNT charge at a standoff distance of 2 m. The intense pressure wave generated by the explosion has significantly deformed the connection, particularly the steel plate and surrounding concrete. High stress concentrations near the blast impact point have led to localized material failure and damage. The steel components exhibit substantial plastic deformation, characterized by large displacements and distorted shapes. The concrete foundation and pedestal are also affected by the blast wave, displaying visible cracks and spalling. The anchor bolts connecting the steel plate to the concrete foundation appear to have experienced significant stress, potentially leading to failure or plastic deformation. Figures 23, 24, 25, and 26 illustrate the generated stresses of the connection from different perspectives.

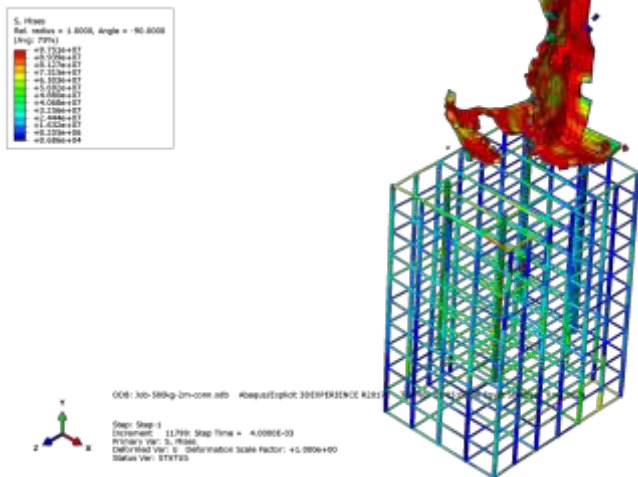


Figures (23): Global stress contour plot for the BPCC Subjected to blast loading for model (D)

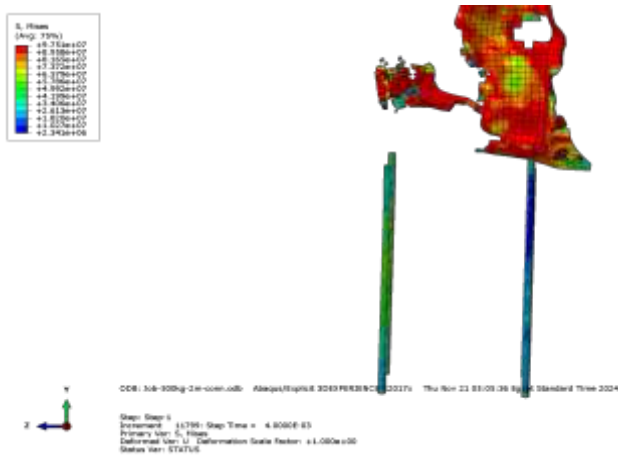


Figures (24): Stress contour plot focusing on

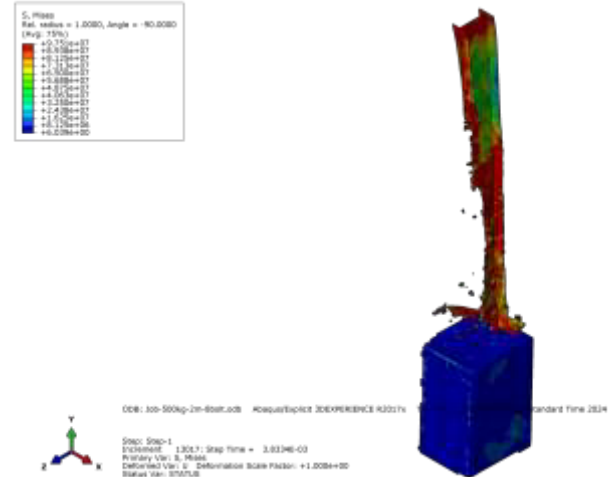
the BPCC connection for model (D)



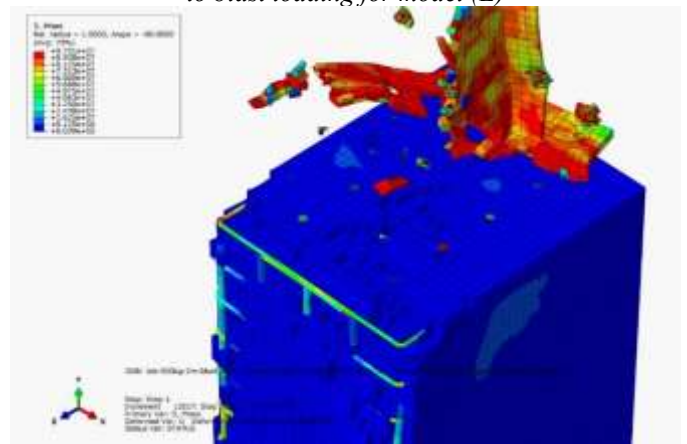
Figures (25): Stress contour plot for the BPCC connection and reinforcement within the concrete for model (D)



Figures (26): Stress contour plot focusing on the anchor bolts for model (D)



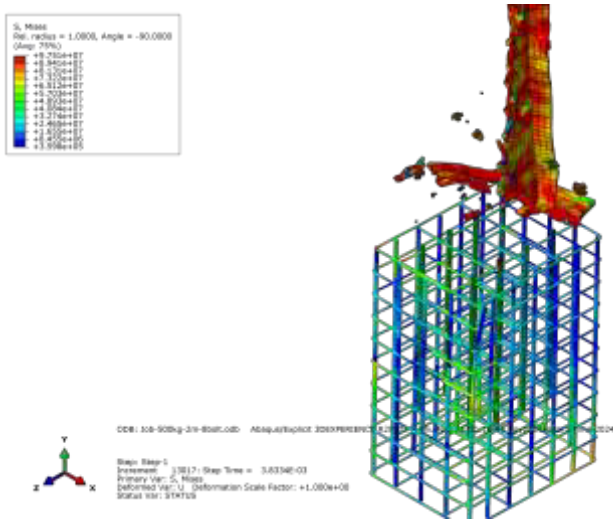
Figures (27): Global stress contour plot for the BPCC Subjected to blast loading for model (E)



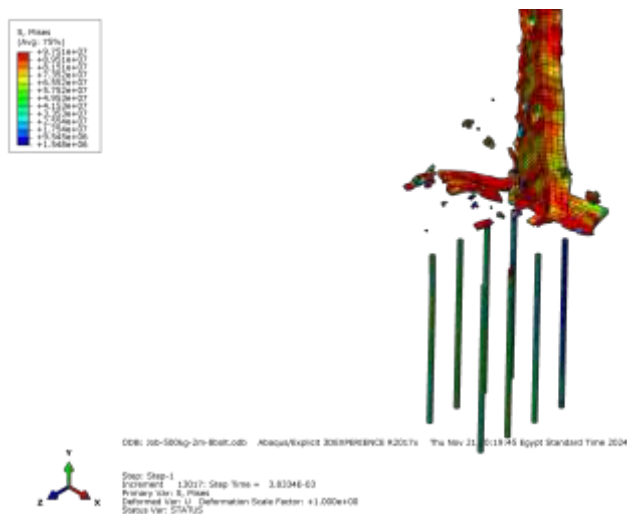
Figures (28): Stress contour plot focusing on the BPCC connection for model (E)

Model (E):

The BPCC was subjected to a blast wave generated by a 500 kg TNT charge at a standoff distance of 2 m. This model was similar to Model D, except for the increased number of bolts from 4 to 8. No significant changes were observed in the stress or deformation patterns within the connection. The results were nearly identical to those of Model D, indicating that increasing the number of bolts had a negligible impact on the connection's response to the blast load. Figures 27, 28, 29, and 30 illustrate the generated stresses of the connection from different perspectives.



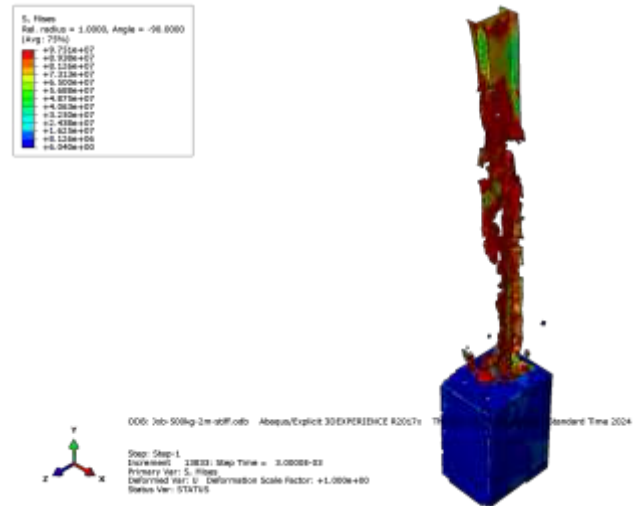
Figures (29): Stress contour plot for the BPCC connection and reinforcement within the concrete for model (E)



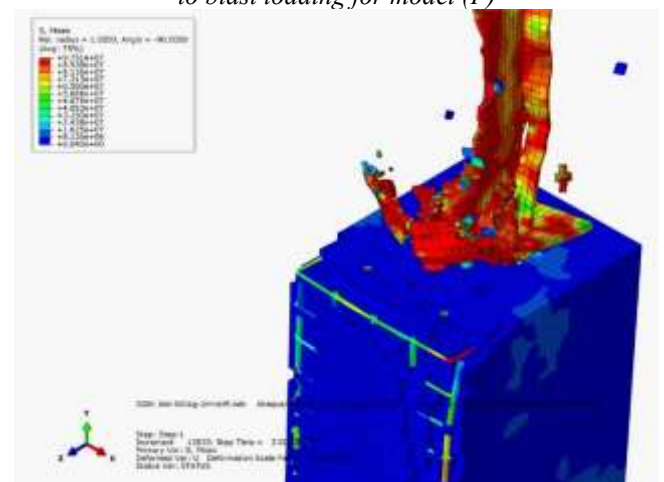
Figures (30): Stress contour plot focusing on the anchor bolts for model (E)

Model (F):

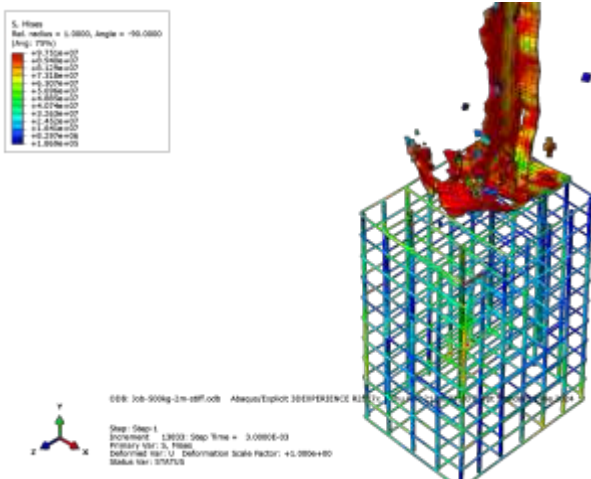
The BPCC was subjected to a blast wave generated by a 500 kg TNT charge at a standoff distance of 2 m. This model was similar to Model D, with the addition of stiffeners. The model exhibited reduced damage to the base plate compared to Model D, although significant damage remained within the connection. Figures 31, 32, 33, and 34 illustrate the stress distribution within the connection from different perspectives.



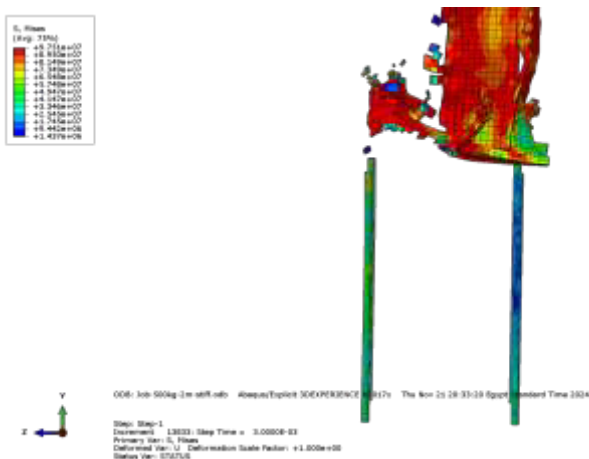
Figures (31): Global stress contour plot for the BPCC Subjected to blast loading for model (F)



Figures (32): Stress contour plot focusing on the BPCC connection for model (F)

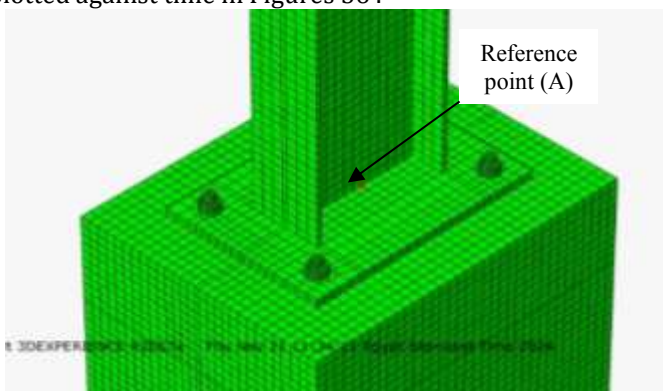


Figures (33): Stress contour plot for the BPCC connection and reinforcement within the concrete for model (F)

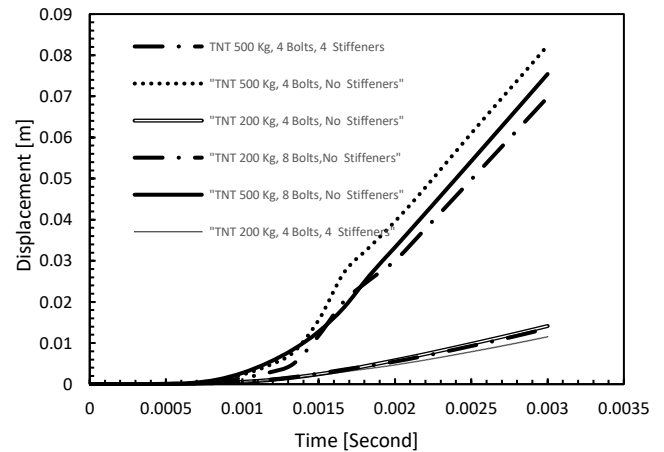


Figures (34): Stress contour plot focusing on the anchor bolts for model (F)

A reference point (A) was selected at the center of the base plate, which is also connected to the column as shown in Figure 35. The deformations at this point were calculated and plotted against time in Figures 36.



Figures (35): The location of the reference point in which stresses and deformations were calculated



Figures (36): The location of the reference point in which stresses and deformations were calculated

VII. CONCLUSION

This study numerically investigated the structural behavior of Column Base Plate-Column Connections (BPCCs) subjected to blast loading. Six different models were analyzed to assess the impact of various parameters, including the magnitude of the explosive charge, standoff distance, bolt quantity, and the presence of stiffeners. The results indicate that increasing the number of bolts had a negligible impact on the overall response of the BPCCs to blast loading. However, the addition of stiffeners proved to be effective in mitigating the damage to the base plate and reducing the deformation of the front bolts. The most significant damage was observed in models subjected to higher explosive charges and shorter standoff distances. These models experienced significant plastic deformation, localized material failure, and damage to the concrete foundation and pedestal.

Future research could explore the effects of different explosive materials, and structural configurations on the response of BPCCs to blast loading. Additionally, experimental validation of the numerical models could further enhance the accuracy and reliability of the predictions.

VII. REFERENCES

- [1] Kim, J., Ghaboussi, J., & Elnashai, A. S. (2010). Mechanical and informational modeling of steel beam-to-column connections. *Engineering Structures*, 32(2), 449-458.
- [2] Shafiee, M., & Amiri, G. R. (2016). Experimental and numerical investigation of the behavior of column base plates with different embedment depths. *Thin-Walled Structures*, 107, 152-162.
- [3] Hassan, A. S., Torres-Rodas, P., Giulietti, L., & Kanvinde, A. (2021). Strength characterization of

- exposed column base plates subjected to axial force and biaxial bending. *Engineering Structures*, 237. doi: 10.1016/j.engstruct.2021.112165.
- [4] Azadeh, M., & Pakzad, M. T. (2014). Experimental and numerical investigation of extended end-plate connections with various stiffener configurations. *Journal of Constructional Steel Research*, 103, 118-129.
 - [5] DeWolf, J. T., & Sarisley, E. F. (1980). *Column Base Plates with Axial Loads and Moments*. *Journal of the Structural Division*, 106(11), 2167–2184. doi:10.1061/jsdeag.0005569.
 - [6] Cormie, D., Mays, G., and Smith, P. (2009). *Blast effects on buildings*, Thomas Telford Ltd., London.
 - [7] Longinow, A., and Alfawakhiri, F. (2003). *Blast resistant design with structural steel*. *Modern Steel Construction*, 43(10), 61-66.

 - [8] Yazdani, N., & Astaneh-Asl, A. (2010). Blast-resistant design of steel structures. *Journal of Constructional Steel Research*, 66(11), 1477-1486.
 - [9] Jaspart, J. P., & Vandegans, D. (1998). *Application of the component method to column bases*. *Journal of Constructional Steel Research*, 48(2–3), 89–106. doi:10.1016/S0143-974X(98)90196-1
 - [10] Abd-El-Latif, A. M., Zahran, F., Nazif, M. A., & Khalifa, S. (2024). *The Behavior of Steel Bolted Beam-Column Connection under Blast Load*. *Fayoum University Journal of Engineering*, 7(2), 38-44.
 - [11] Abd-El-Nabi, E., Zahran, F., & Selouma, T. (2024). Numerical Analysis of Reinforced Concrete Columns Strengthened with Steel Jacket. *Fayoum University Journal of Engineering*, 7(2), 21-30.
 - [12] GR, J. & WH., C., 1983. A constitutive model and data for metals subjected to large strains, high strain rates, and high temperatures. The Hague Netherlands.